



OPEN Cultivation of Nordic *Chlorococcum* sp. in anaerobic digestion effluent: Effects of CO₂ concentration and reactor configuration

Ghasem Mohammadkhani^{1✉}, Amir Mahboubi¹, Christiane Funk² & Päivi Ylittervo¹

The increasing discharge of untreated wastewater poses risks to ecosystems and public health, necessitating sustainable treatment strategies. Anaerobic digestion (AD) of sewage sludge offers several benefits including waste-volume reduction and sludge stabilization. However, it produces nutrient-rich effluents, requiring further treatment. Microalgae can remove nutrients while generating valuable biomass. This study aimed to evaluate the effect of CO₂ concentration and reactor configuration on the performance of *Chlorococcum* sp. cultivated in AD effluent of municipal sewage sludge. Four CO₂ levels (0.04, 3, 6, and 9%) was tested and 6% CO₂ yielded the highest biomass (0.98 g L⁻¹) and CO₂ fixation rate (162 mg L⁻¹ d⁻¹), while maintaining ammonium and phosphorus removal comparable to aeration with 3 and 9% CO₂. This concentration was used in ALR, BC, and BC with carriers. The highest nutrient removal was achieved in BC, with 37.61% NH₄⁺-N and 25.87% phosphorus reduction, whereas growth in ALR reached the highest cell density (81 × 10⁶ cells mL⁻¹) in 9 days. Biomass composition was stable across reactors, with similar protein, carbohydrate, or fatty acid methyl esters content. These findings demonstrate that the Nordic *Chlorococcum* sp. grown in AD effluent can remove NH₄⁺-N and phosphorus across a wide CO₂ range (0.04–9%). Culturing in ALR is the preferred option for rapid growth. However, BC offered better nutrient removal and higher biomass production but required longer cultivation than ALR.

Keywords CO₂ concentration, reactor configuration, *Chlorococcum* sp., anaerobic digestion effluent

The increasing release of untreated wastewater due to urban growth and industrial activities endangers aquatic environments and human health, primarily through contamination with heavy metals, organic compounds, and pathogens¹. As freshwater resources decline and global water consumption is projected to rise by 55% by 2050², the recycling and reuse of wastewater has become urgent. Untreated effluents lead to eutrophication and waterborne diseases, making effective wastewater treatment essential for safeguarding ecosystems and ensuring sustainable water use^{1,3}. Anaerobic digestion (AD) of sewage sludge is a widely adopted method that can address this issue by transforming organic materials into biogas and removing harmful pathogens. This not only reduces health hazards associated with sludge disposal but also yields an effluent rich in nutrients⁴. However, additional treatment is necessary for this effluent to comply with discharge regulations, mainly for ammonium nitrogen⁵.

Microalgae offer an effective biological approach to wastewater treatment by assimilating nitrogen and phosphorus⁶, reducing contaminants such as heavy metals and chemical oxygen demand (COD)⁷. Moreover, microalgae generate biomass that can be used for various valuable applications such as biofuels, biofertilizers, biostimulants^{8,9}, biopolymers¹⁰, or biochar¹¹. Due to their minimal energy requirements and strong potential for resource recovery, microalgae-based technologies are both cost-effective and environmentally friendly. Their integration with AD effluent enhances nutrient removal and supports a circular bioeconomy¹².

CO₂ is an essential carbon source for photosynthesis, and both microalgal growth and biomass production are strongly influenced by CO₂ concentration. However, excessively high CO₂ concentrations may inhibit photosynthesis and reduce growth owing to significant pH reduction, highlighting the importance of identifying optimal CO₂ levels¹³, which are strain-dependent because each microalgal strain shows unique tolerance and performance thresholds. For example, *Chlorella vulgaris* has been reported to achieved a maximum biomass concentration of 2.12 g L⁻¹ at 10% CO₂¹⁴, whereas *Chlorella pyrenoidosa* attained its highest biomass concentration of 4.3 g L⁻¹ under 5% CO₂¹⁵. In another study, Harwati, Willke and Vorlop¹⁶ reported that

¹Swedish Centre for Resource Recovery, University of Borås, Borås 50190, SE, Sweden. ²Department of Chemistry, Umeå University, Umeå 901 87, SE, Sweden. ✉email: ghasem.mohammadkhani@hb.se

Chlorococcum sp. demonstrated optimal growth and lipid accumulation when aerated with 6% CO₂, but showed reduced cell density and total lipid content at 10%, indicating a threshold beyond which further CO₂ enrichment may hinder performance. Furthermore, elevated CO₂ levels could induce metabolic shifts, leading to increased lipid and carbohydrate accumulation^{15,17}.

Another important parameter that directly affects photosynthetic efficiency and microalgal growth is CO₂ availability for the cells, which can be constrained by suboptimal mass transfer such as short residence times of CO₂ bubbles and limited mixing. In photobioreactors, CO₂ is typically sparged into the system as bubbles. Bubbles size and behavior affect gas distribution and transfer efficiency, ultimately impacting microalgal biomass productivity¹⁸. For instance, techniques such as hollow fiber membranes (HFMs) for bubble-less gas exchange have been shown to improve CO₂ delivery and biomass accumulation¹⁹. The efficiency of CO₂ mass transfer is influenced by factors such as gas distributor design, sparger orifice diameter and spacing, which can increase CO₂ retention time in the liquid phase and improve mass transfer coefficients²⁰. On the other hand, transfer of CO₂ and O₂ is often limited by reactor geometry and operational parameters. Additionally, optimizing gas distributor design and flow rates can enhance CO₂ dissolution and mixing, leading to better growth and carbon fixation^{20,21}. Therefore, reactor design plays a critical role in addressing these limitations. Airlift Reactor (ALR) features a regular cyclic flow pattern that enhances light conversion efficiency and photosynthetic performance, supported by a centric-tube column that promotes effective mixing and uniform light distribution, resulting in higher cell concentrations and growth rates^{22,23}. In contrast, the Bubble Column Reactor (BC) shows a more random fluid motion characterized by low-frequency circular loops²², which is expected to result in less efficient mixing and suboptimal nutrient and light availability, ultimately yielding lower photosynthetic productivity²³. However, the incorporation of carriers into BC reactors significantly improves their performance by providing surfaces for microalgae attachment, thereby enhancing nutrient uptake and biomass yield²⁴. Additionally, they enhance gas-liquid mass transfer, increasing CO₂ utilization and fixation rates, which further boosts microalgal growth^{24,25}. They can also increase the CO₂ residence time in the liquid phase to enhance the CO₂ removal efficiency²⁶.

Given the importance of optimizing CO₂ concentration and reactor configuration to enhance microalgal performance, a systematic evaluation of these parameters is essential. Reactor design not only influences gas transfer and mixing but also determines nutrient uptake and biomass characteristics. Building on these insights, this study first evaluated four different CO₂ supplementation levels (0.04, 3, 6, and 9%) to identify the optimal range for nutrient removal and microalgae growth of Nordic *Chlorococcum* sp. The selected supplementation level was then used for microalgae cultivation in three different photobioreactor designs (ALR, BC, and BC with carriers) to assess the impact of reactor design on nutrient and CO₂ removal efficiency, biomass production, and biomass composition. The microalgae strain was the Nordic strain *Chlorococcum* sp. which has not previously been evaluated for the growth performance in anaerobic digestion effluent derived from municipal sewage sludge. Finally, this research directly advances several United Nations Sustainable Development Goals (SDGs). It contributes to SDG 13 (Climate Action) and SDG 14 (Life Below Water) by mitigating greenhouse gas emissions and reducing the risk of eutrophication. It also supports SDG 6 (Clean Water and Sanitation) by nutrient removal from AD effluent.

Materials and methods

Microalgae medium

Borås Energy and Environment (Borås, Sweden) supplied the liquid fraction from AD of municipal sewage sludge. The initial effluent pH was 8.1–8.3. It was first filtered using a 10 µm pore-size filter paper (Ahlstrom-Munksjo Munktell, Thermo Fisher Scientific, Sweden) and then diluted with Milli-Q water to adjust the ammonium nitrogen concentration to approximately 240 mg L⁻¹, based on the optimal level identified in our previous study²⁷. The diluted effluent was subsequently autoclaved, which raised the pH to 8.8–9.1, and was used as the cultivation medium for microalgae without any further pH adjustment. The nutrient and elemental composition of the filtered AD effluent is presented in Table 1, which was kept at -20 °C until the experiment.

Algal cultivation

The Nordic microalgal strain *Chlorococcum* sp. (MC-1) was originally isolated from a freshwater lake in Bäckhammar, located in west-central Sweden²⁸. To prepare the pre-culture, *Chlorococcum* sp. was grown in sterile BG-11 medium in 500 mL Erlenmeyer flasks, with a working volume of 170 mL, sealed with cotton plugs

	Concentration (mg L ⁻¹)		Concentration (ppm)
NH ₄ ⁺ -N	237.91 ± 11.11	Mg	4.85 ± 0.19
NO ₃ -N	2.14 ± 0.23	Fe	2.14 ± 0.23
NO ₂ -N	0.05 ± 0.00	Na	78.5 ± 1.50
PO ₄ ⁻³	9.28 ± 0.56	K	24.85 ± 0.22
Total P	4.14 ± 0.10	Cu	0.15 ± 0.01
sCOD ^a	535.36 ± 19.25	Co	0.06 ± 0.01

Table 1. Nutrient and elemental composition of growth medium on day 0 of cultivation. ^a Soluble chemical oxygen demand.

on an open-air shaker (New Brunswick, UK) at 120 rpm at 25 °C, and exposed to continuous white light at an intensity of $80 \mu\text{mol m}^{-2} \text{s}^{-1}$. BG11 was prepared as described previously²⁷, and the pH of BG11 was adjusted to 7.1 using 1 M HCL. Light intensity was monitored using an SKP 200 PAR Quantum Sensor (Skye Instruments, UK).

A five-day old algal culture was used for inoculation to achieve an optical density (OD_{750}) of 0.1 for all experimental conditions. This study was conducted in two stages. In the first stage, the effects of different CO_2 concentrations, including 0.04 (air), 3, 6, and 9%, on microalgal growth and nutrient removal were evaluated. All cultivations during this phase were performed in BC reactors. In the second stage, the reactor configuration was investigated using the optimal CO_2 concentration identified in stage one (6% CO_2 mixed with air). Three reactor setups were tested: a standard BC, an ALR, and a BC with carriers (AnoxKaldnes K1-type carriers, AnoxKaldnes, Lund, Sweden) as presented in Fig. 1, and the BC with carriers was labeled as carrier in the tables and figures.

In this study, the cultivation was conducted in 4.5 L capacity glass BC bioreactors (56 cm height and 11 cm width, Belach Bioteknik AB, Skogås, Sweden). Each bioreactor was initially filled with 2.5 L of AD effluent and autoclaved at 121 °C for 20 min. After sterilization, an appropriate volume of pre-culture was added to reach OD_{750} of 0.1. The initial ammonium nitrogen concentration and working volume of each reactor were approximately 240 mg L^{-1} and 3.5 L.

The ALR configuration was similar to the BC design but included a centered glass draft tube (40 cm height and 6 cm width). For the BC with carriers, approximately 150 g of carrier material (1 cm height, 0.5 cm width) was added, equivalent to 150 mL of liquid volume displacement.

All cultures were continuously bubbled with either air or air enriched with CO_2 (3, 6, or 9% v/v) at a constant flow rate of 500 mL min^{-1} . Illumination was provided by continuous white light at an intensity of $100 \mu\text{mol m}^{-2} \text{s}^{-1}$. To prevent contamination, the gas mixtures were filtered through $0.3 \mu\text{m}$ Whatman HEPA-VENT filters (Cytiva, USA) before entering the reactor. All experiments were performed in biological duplicates over a 12-day cultivation period.

Microalgal growth

Every two days, a 1 mL sample was taken from each reactor to measure the optical density, cell count, and pH. The optical densities at 530, 680, and 750 nm were assessed using a visible spectrophotometer (Thermo Scientific™ GENESYS 140 Visible Spectrophotometer, Sweden). CellDrop FL (Denovix, USA, Denovix [30]) was used to determine the number of cells mL^{-1} , and the pH was assessed using a pH meter (METTLER TOLEDO, Switzerland). Samples with optical densities exceeding 1 were diluted; otherwise, the optical density was measured directly. A 10 ml sample was collected daily and centrifuged for 5 min at $3000 \times g$. The biomass was then washed twice with Milli-Q water to eliminate any residual components. Dry weight was measured gravimetrically [31]. At the end of the cultivation period, the cultures were harvested and washed twice with Milli-Q water. Subsequently, the biomass was freeze-dried using equipment from Labconco, USA.

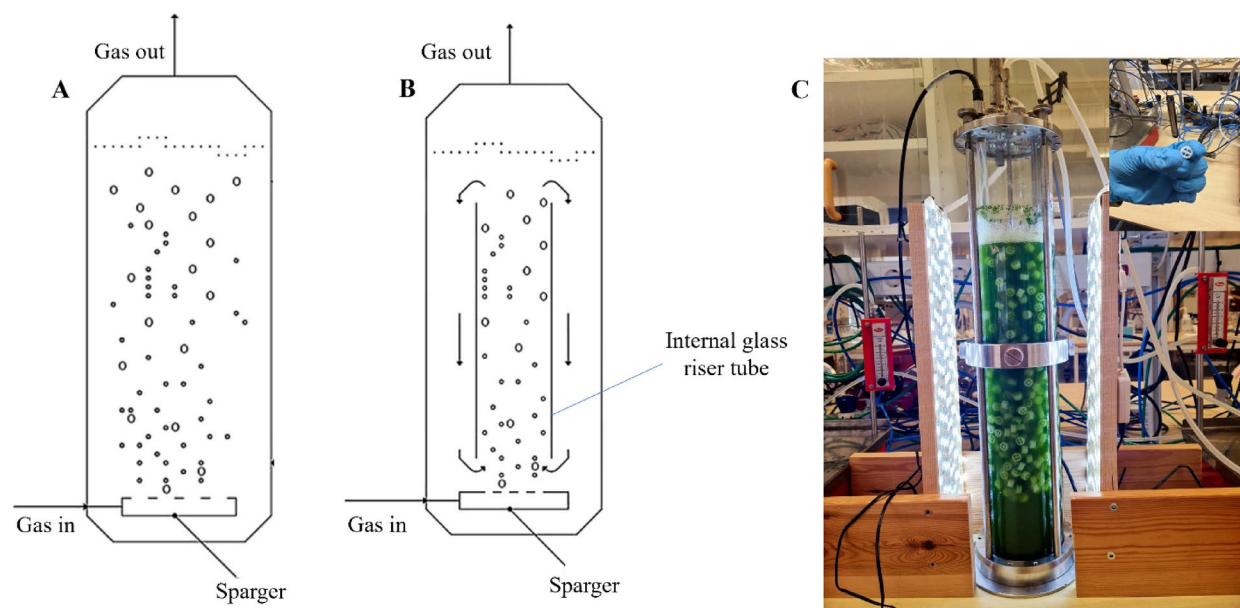


Fig. 1. Schematic representation of the bubble column bioreactor (A) and airlift bioreactor (B). Bubble column bioreactor with carriers (C). Pictures A and B were adapted from²⁹, with Permission from Elsevier.

Analytical methods

The concentrations of total soluble chemical oxygen demand (sCOD), $\text{NH}_4\text{-N}$, $\text{NO}_3\text{-N}$, $\text{NO}_2\text{-N}$, PO_4 and total P were measured using COD 15,000, ammonium 100, Nitrite 2, standard test nitrate and nitrate 250, ortho- and total-Phosphate 15, respectively (Nanocolor® Düren, Germany). A Nanocolor 500D photometer (MACHEREY-NAGEL GmbH & Co. KG, Germany) were used to assess the levels of these parameters.

The elements Fe, Mg, Ca, Na, K, Cu, and Co were quantified using Microwave Plasma-Atomic Emission Spectroscopy (MP-AES, Agilent Technologies, USA). All analyses were performed in duplicate.

To analyze the fatty acid compositions, a direct transesterification technique (D-TE) was employed, as described by Cavonius, Carlsson and Undeland [32]. Following this, the extracted fatty acid methyl ester (FAME) was subjected to gas chromatography (GC) analysis. For this purpose, a GC-FID (Perkin Elmer, Clarus 590) with a DB-23 column (Agilent, USA) was employed to examine the FAME. Nitrogen at a flow rate of 0.64 mL min^{-1} served as the carrier gas, and the GC operated under a constant pressure of 94.45 kPa. Initially, the oven was heated to $50 \text{ }^\circ\text{C}$ for 2 min. The temperature then increased at a rate of $12 \text{ }^\circ\text{C min}^{-1}$ until it reached $175 \text{ }^\circ\text{C}$, followed by a slower ramp of $2 \text{ }^\circ\text{C min}^{-1}$ until it attained $230 \text{ }^\circ\text{C}$, which was held for 11 min.

Crude fat was extracted from solid samples using an ST 255 Soxtec™ extractive system (FOSS, Hillerød, Denmark). Approximately 1 g of dried material was placed in a cellulose thimble and loaded into the device, where petroleum ether served as the solvent in a three-step extraction procedure consisting of 15 min boiling, 30 min rinsing, and a 10 min solvent removal phase. The recovered extractives were collected in an aluminum cup, oven-dried overnight at $70 \text{ }^\circ\text{C}$, and quantified gravimetrically. The results were reported as a percentage of the original sample weight.

To determine the protein content in the microalgal biomass, the total nitrogen content was initially assessed and then converted into protein content by applying a conversion factor of 4.78 [33]. The Element Analyzer FlashSmart CNHS (Thermo Fisher Scientific, USA) was employed to assess the total nitrogen and carbon content in microalgal biomass, with nitrogen being identified using a thermal conductivity detection system. Each tin capsule was filled with 3 to 4 mg of the sample (freeze-dried biomass) and placed in an autosampler. The combustion reactor was set to $950 \text{ }^\circ\text{C}$, and the GC oven was maintained at $65 \text{ }^\circ\text{C}$. Helium served as the carrier gas at a flow rate of 140 mL min^{-1} , and pure oxygen was used as the combustion gas at a flow rate of 250 mL min^{-1} . C/N ratios were determined using data from the elemental analyzer.

To assess the total carbohydrate content in microalgal biomass, a detailed standard operating procedure suggested by Chen, Gao, Song, Sommerfeld and Hu [34] was used. The carbohydrate content was determined by comparing their absorbance values at 490 nm against a glucose calibration curve created from known glucose concentrations.

Ash content was determined using a TGA/DSC 3+ analyzer (Mettler-Toledo, Switzerland) with a thermal profile adapted from Swedish standard (SS 187187). Samples (10 to 15 mg) were analyzed in alumina crucibles under a constant air flow of 50 mL min^{-1} . The program involved drying at $105 \text{ }^\circ\text{C}$ (30 min), ramping to $550 \text{ }^\circ\text{C}$ (60 min), holding at $550 \text{ }^\circ\text{C}$ (60 min), followed by cooling to ambient temperature (60 min). Ash content was calculated from the blank-corrected residual mass at the end of the isothermal hold, normalized to the initial dry mass.

CO_2 biofixation rate

Biomass productivity (P , $\text{mg L}^{-1} \text{ d}^{-1}$) was calculated from the change in biomass concentration over time, as shown in Eq. (1):

$$P = \frac{X_1 - X_0}{t_1 - t_0} \quad (1)$$

Where X_1 and X_0 represent the biomass concentration at times t_1 and t_0 , respectively. In this study, t_0 and t_1 were set at day zero and 12, respectively.

The carbon dioxide biofixation rate (R_C , $\text{mg}_{\text{CO}_2} \text{ L}^{-1} \text{ d}^{-1}$) was calculated using Eq. (2):

$$R_C = C_C \times P \times \left(\frac{M_{\text{CO}_2}}{M_C} \right) \quad (2)$$

Where P is the biomass productivity, and C_C is the carbon content of the biomass determined by elemental analysis. M_{CO_2} and M_C are the molar mass of carbon dioxide and carbon, respectively. This approach follows established methods reported in the literature [35,36].

Statistical analysis

All the biological experiments were conducted in duplicate. Each type of analysis, such as GC analysis, cell counting, pH measurement, OD measurement, elemental analysis, MP-AES, and test kit assessments, was performed in two replicates. Statistical analyses were carried out using Minitab® 21 (Minitab Ltd., Coventry, UK). The responses were assessed using analysis of variance (ANOVA), and pairwise comparisons were performed using Tukey's test with a 95% confidence interval. The data presented are the averages of the obtained values, and the error bars in the text, tables, and graphs indicate the standard deviations.

Results and discussion

Effect of CO_2 concentration on microalgae growth

In the first stage of this study, *Chlorococcum* sp. was cultivated in a BC bioreactor using AD effluent from municipal sewage sludge supplemented with different concentrations of CO_2 (0.04, 3, 6, and 9%). The biomass

dry weight, optical density, and pH values of *Chlorococcum* sp. cultures under different CO₂ concentrations with a cultivation time of 12 days are presented in Fig. 2. The pH range measured for 0.04, 3, 6, and 9% CO₂ (average value of day 1 to 12) was 8.91 ± 0.03 , 7.51 ± 0.04 , 7.18 ± 0.05 , 6.87 ± 0.08 , respectively, indicating that increasing the CO₂ supply from 0.04 to higher CO₂ percentages reduced the pH values. When carbon dioxide is dissolved in water, algae cells can utilize it in photosynthesis. While active photosynthesis leads to an increased pH value in the medium, increased concentrations of CO₂ reduce the pH as any CO₂ not used in biomass production is transformed into carbonic acid (H₂CO₃). The most favorable CO₂ concentration for growth of *Chlorococcum* sp. was 6%, contributing to the highest biomass yield of 0.98 ± 0.01 g L⁻¹. This condition also achieved significantly higher optical densities (p value of $0.026 < 0.05$) in 12 days compared to the 9% concentration, and this result is in line with the data reported by Harwati, Willke and Vorlop [16]. Supplementing the culture with 6% CO₂ resulted in a 4.6 fold increase in the final biomass concentration compared to cultivation with 0.04% CO₂, which yielded

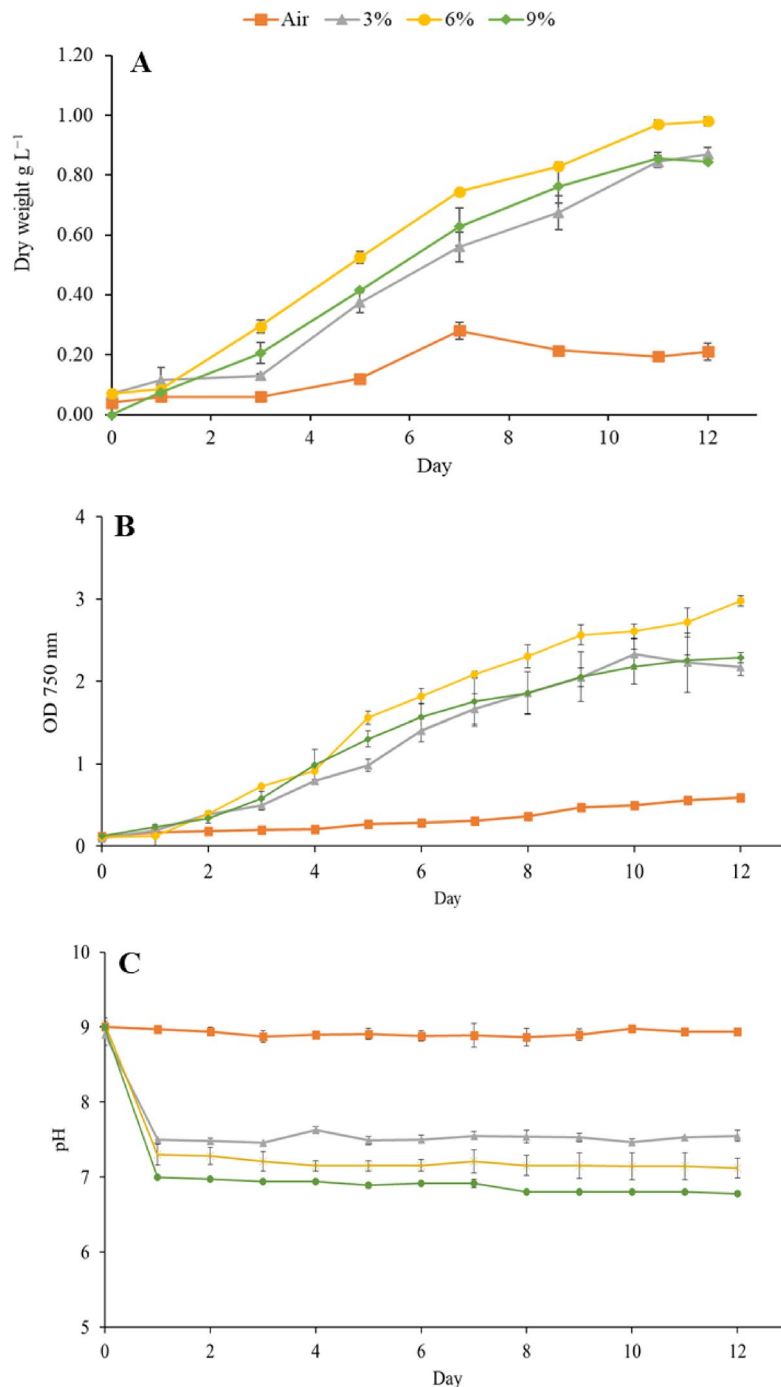


Fig. 2. Biomass dry weight (A), optical densities (OD750 nm) (B), and pH changes (C) of *Chlorococcum* sp. cultures cultivated in anaerobic digestion effluents under different CO₂ concentrations.

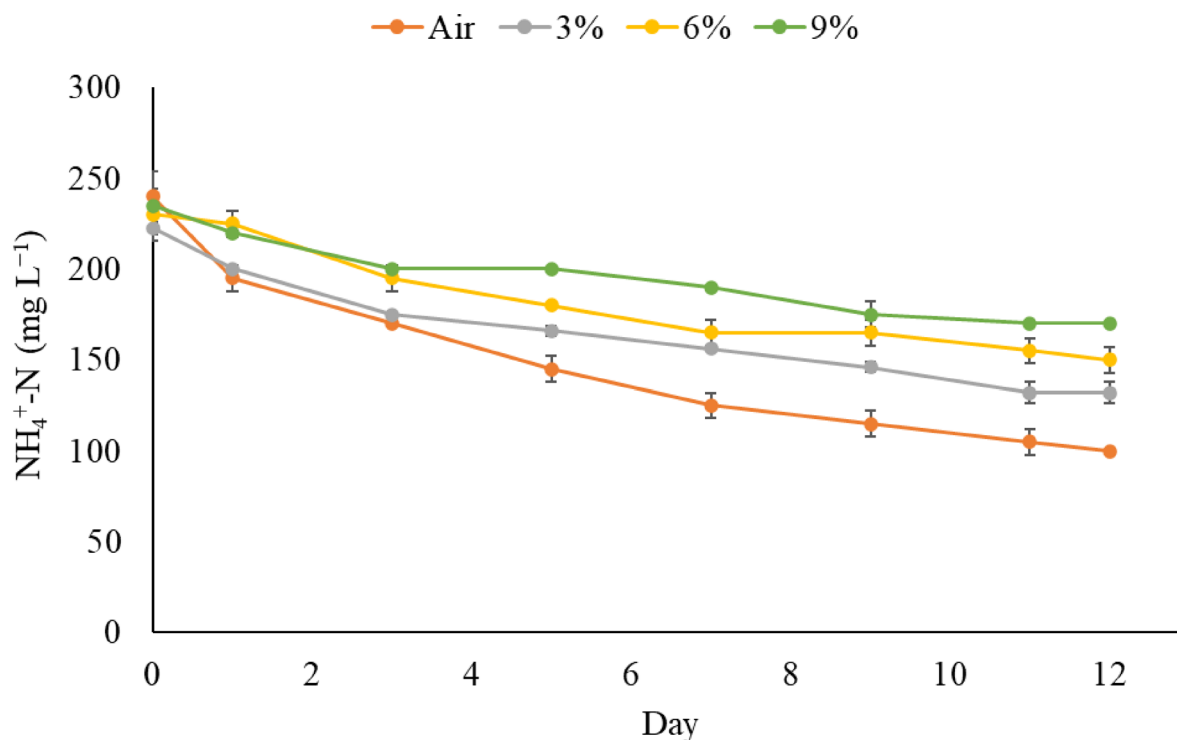


Fig. 3. Ammonium nitrogen removal by *Chlorococcum* sp. cultures cultivated in anaerobic digestion effluents under different CO₂ concentrations.

CO ₂ (%)	Removal efficiency (%)		Productivity	CO ₂ fixation rate
	NH ₄ ⁺ -N	P	mg biomass L ⁻¹ d ⁻¹	mg CO ₂ L ⁻¹ d ⁻¹
0.04	58.04 ± 4.94 ^a	40.06 ± 2.49 ^a	14.58 ± 2.94 ^a	27.05 ± 5.44 ^a
3	40.64 ± 3.48 ^b	25.48 ± 4.93 ^b	66.66 ± 1.17 ^b	146.42 ± 2.24 ^{bc}
6	34.56 ± 7.09 ^c	22.01 ± 0.43 ^b	76.25 ± 0.58 ^b	162.55 ± 2.28 ^b
9	27.62 ± 2.17 ^c	16.81 ± 3.21 ^b	66.66 ± 0.00 ^b	140.35 ± 5.34 ^c

Table 2. Nutrient removal efficiency, biomass productivity and CO₂ fixation rate under different CO₂ concentrations. Values followed by different letters within the same column are significantly different (p value < 0.05).

in the lowest biomass concentration (0.21 ± 0.03 g L⁻¹) possibly due to limited photosynthesis compared to CO₂ enriched conditions [37]. Furthermore, the medium pH was around 9 that is potentially outside the preferred pH range for *Chlorococcum* sp. This high pH was likely inhibitory due to its effect on the dissolved inorganic carbon equilibrium. This equilibrium balances dissolved CO₂ (dominant if pH < 6.3), bicarbonate (HCO₃⁻, dominant if 6.3 < pH < 10.3), and carbonate (CO₃²⁻, dominant if pH > 10.3) and at pH 9 the equilibrium is dominated by bicarbonate, while the concentration of dissolved CO₂ is negligible. Although the carbon is not yet locked as carbonate at this stage (carbonate only becomes significant above pH 10), the complete absence of free dissolved CO₂ and the highly alkaline conditions likely created a suboptimal environment for growth, which slow photosynthesis and enhances respiration [38]. Even though some *Chlorococcum* species can tolerate pH values between 5 and 9 [39], the optimal pH for *Chlorococcum* sp. is neutral to moderately alkaline, pH 7.3 to 8.5 [16,40]. The poor growth at pH 9 aligns of the Nordic *Chlorococcum* sp. used here supports reports of its lower pH optimum [16]. Notably, exposure to 9% CO₂ did not lead to higher biomass production than 3% or 6%, which may be caused by the lower pH values in 9% (6.76 < pH < 6.99) compared to 3% CO₂ (7.46 < pH < 7.63).

Effect of CO₂ concentration on nutrient and CO₂ removal

Figure 3 presents the ammonium nitrogen removal for different CO₂ concentrations over 12 days. A 0.04% CO₂ aeration resulted in significantly higher NH₄⁺-N removal (58.04%) than those enriched with carbon dioxide, which is consistent with our previous findings. Furthermore, this condition resulted in the highest phosphorus removal rate (40.06%; Table 2).

Growth in the presence of 3% CO₂ resulted in significantly higher NH₄⁺-N removal efficiency than 6% or 9% CO₂ (Table 2), while 6% CO₂ did not result in a significantly different NH₄⁺-N removal efficiency than 9% CO₂.

The nutrient removal efficiencies observed in this study (27–58% $\text{NH}_4^+\text{-N}$ and 16–40% P removal) are within the lower to mid-range of values reported for microalgae cultivated in municipal wastewater. Higher removal efficiencies (50–85% for N and P) have been reported in large-scale tubular or raceway systems treating centrate or pre-treated municipal wastewater [41,42]. High-rate algal ponds have also achieved 76% TN and 85% TP removal when strong algae–bacteria synergy is present [43]. However, these systems typically operate at much larger volumes and longer retention times. In another study [44], *Chlorella vulgaris* cultivated under aeration rates of 1.4 to 2.3 vvm in annular airlift and bubble-column photobioreactors showed relatively low nitrogen removal, with $\text{NH}_4^+\text{-N}$ consumption ranging from 16 to 19% during the initial nitrogen-sufficient stage and 30–38% during the nitrogen-reduction phase.

As illustrated in Table 2, the CO_2 fixation rate of *Chlorococcum* sp. under CO_2 enriched conditions was in the range of 140 to 162 $\text{mg L}^{-1} \text{d}^{-1}$. The highest CO_2 fixation rate of 162 $\text{mg L}^{-1} \text{d}^{-1}$ was observed with 6% CO_2 aeration, while the lowest was noted in air aeration (27 $\text{mg L}^{-1} \text{d}^{-1}$). The maximal CO_2 fixation rate obtained under 6% CO_2 conditions exceeded values earlier reported by the authors for *C. vulgaris* (121 $\text{mg L}^{-1} \text{d}^{-1}$) or *Chlorococcum* sp. (99 $\text{mg L}^{-1} \text{d}^{-1}$) under 3% CO_2 . Nonetheless, it is lower than the one reported by Nayak, Karemore and Sen [45] for *Scenedesmus* sp., which exceeded 279 $\text{mg L}^{-1} \text{d}^{-1}$ under 1, 2.5, 5 or 10% CO_2 supply.

All cultivations were performed in duplicates in different reactors. Moreover, growth medium (without any microalgae) was tested as control samples (duplicate) to be able to exclude the effect of ammonia stripping under air aeration conditions. The initial $\text{NH}_4^+\text{-N}$ concentration in the control samples of $242.5 \pm 17.68 \text{ mg L}^{-1}$ decreased to $152.5 \pm 3.54 \text{ mg L}^{-1}$, resulting in a removal efficiency of $36.99\% \pm 3.13\%$. pH values in the control sample ranged from 8.8 to 9.0. At this pH of 8.9 (average), the equilibrium between NH_3 and NH_4^+ shifts to approximately 30.9% NH_3 and 69.1% NH_4^+ , suggesting that part of the ammonium removal was due to conversion to ammonia followed by ammonia stripping under air aeration conditions.

Effect of CO_2 concentration on biomass composition

The fatty acid composition, total fatty acid methyl esters (FAMES), protein, carbohydrate, C/N ratio, and ash content of *Chlorococcum* sp. after growth for 12 day under different CO_2 concentrations are shown in Table 3. The protein content (38.76–43.73%) and carbohydrate content (9.13–13.17%) in *Chlorococcum* sp. were stable under different aeration conditions, with the highest protein production of 43.73% under 0.04% CO_2 and the highest carbohydrate production of 13.17% under 9% CO_2 . However, the total FAMES percentage ranged from 2.88% (0.04% CO_2) to 34.48% (9% CO_2) of the biomass dry weight. The highest FAMES production was achieved by 9% CO_2 aeration, followed by 6, 3 and 0.04%, respectively.

This pattern indicates that an increased supply of CO_2 promotes greater fatty acid production. To explain further, elevated CO_2 enhances carbon fixation through the Calvin cycle, increasing the intracellular availability of carbon precursors such as acetyl-CoA and malonyl-CoA. These compounds are required for the cell to synthesize new fatty acids from scratch (de novo synthesis) rather than relying on modification of existing lipids. Higher CO_2 availability can also shift cellular metabolism toward storage compounds such as lipids. Although our study did not directly quantify metabolic intermediates or enzyme activities, the observed increase in FAMES is consistent with these established physiological responses, which is consistent with the findings of Harwati, Willke and Vorlop [16], who observed increased lipid content in *Chlorococcum* sp. at CO_2 aeration levels of 1, 3 and 6% compared to 0.04%. Moreover, Sun, Dou, Wu, He, Wang and Chen [46] investigated the effects of aeration with CO_2 concentrations ranging from 1% to 10% on the growth of *Chlorella sorokiniana*. Their findings showed that using 10% CO_2 aeration significantly enhanced the lipid content compared to other tested concentrations (0.04, 1, 2 and 5%).

In this study, the primary fatty acid methyl esters of *Chlorococcum* sp. included C16:0 (palmitic acid), C18:1 (oleic acid), C18:2 (linoleic acid), and C18:3 (linolenic acid), with a smaller proportion of C16:1 (palmitoleic acid) and C18:0 (stearic acid). Other fatty acids were either not detected in the chromatograms or were present

Fatty acid profile (%)	CO_2 (%)			
	0.04	3	6	9
C16:0 (palmitic acid)	19.01 ± 0.17	17.93 ± 0.57	18.12 ± 0.09	17.94 ± 0.01
C16:1 (palmitoleic acid)	1.20 ± 0.40	0.38 ± 0.14	0.51 ± 0.00	0.19 ± 0.02
C18:0 (stearic acid)	0.00 ± 0.00	0.05 ± 0.01	0.14 ± 0.01	0.19 ± 0.01
C18:1 (oleic acid)	7.61 ± 0.03	40.83 ± 4.08	32.01 ± 0.32	37.82 ± 0.04
C18:2 (linoleic acid)	20.18 ± 0.29	21.2 ± 3.32	27.4 ± 0.30	26.7 ± 0.01
C18:3 (linolenic acid)	39.86 ± 0.79	13.12 ± 0.47	14.94 ± 0.01	11.67 ± 0.01
Biomass (% of dry weight)				
Total FAMES	2.88 ± 0.06	9.79 ± 0.62	28.59 ± 2.39	34.48 ± 1.32
Protein	43.73 ± 0.33	41.58 ± 1.35	40.27 ± 0.98	38.76 ± 0.54
Carbohydrate	9.69 ± 1.00	11.44 ± 0.33	9.13 ± 1.14	13.17 ± 0.42
C/N ratio	5.62 ± 0.02	6.88 ± 0.24	6.90 ± 0.01	7.07 ± 0.17
Ash	7.92 ± 0.09	2.12 ± 0.35	2.81 ± 0.42	1.99 ± 0.19

Table 3. Fatty acid profile, total FAMES, protein, carbohydrate, C/N ratio, and ash content of the dry biomass under different CO_2 concentrations after 12 days of cultivation.

only in trace amounts below the GC-FID detection limit and therefore could not be reliably quantified. The concentration of CO₂ aeration not only affects the quantity of total fatty acids but also affects the fatty acid profile. CO₂ supplementation contributed to a shift from the production of dominantly polyunsaturated fatty acids (PUFAs: containing multiple carbon-carbon double bonds), specifically C18:3, to monounsaturated fatty acids (MUFAs, containing only a single double bond), such C18:1. At 0.04% CO₂ level, the fatty acid profile was dominated by PUFAs, specifically C18:3 with 39.86%, followed by C18:2 with 20.18%. The primary MUFA, C18:1, was present at a relatively low concentration (7.61%), while the saturated fatty acid (SFA, containing no double bonds) C16:0 accounted for 19.01% of the total FAMES. Under supplementation with CO₂ (3, 6 and 9%), a sharp decrease in C18:3 content was observed, which dropped from nearly 40% to 13.12% (at 3% CO₂), 14.94% (at 6% CO₂), and 11.67% (at 9% CO₂). This decrease in PUFAs was directly mirrored by a substantial increase in MUFA C18:1, which increased from 7.61% to a peak of 40.83% at 3% CO₂. This result is consistent with the findings of Li, Trigani, Zuñiga, Eng, Chen, Zengler and Betenbaugh [47], who reported that *C. vulgaris* produced higher levels of C18:1 under 10% and 15% CO₂, and increased C18:3 content when aerated with 0.04% CO₂. Although C18:2 showed a moderate increase, C16:0 remained stable, showing no significant change across all CO₂ concentrations. The C16:1 content, which was already low at 0.04%, decreased further to negligible levels under higher CO₂. These data strongly suggest a metabolic shift from synthesizing building materials (membrane lipids) to storing energy reserves (storage lipids), all driven by carbon availability. Under carbon-limiting conditions (0.04% CO₂), the organism must prioritize the use of every available carbon atom to build essential building materials, such as photosynthetic membranes (thylakoids), required to capture more energy. Therefore, the profile was dominated by PUFA C18:3, a key component of these membranes [48]. In contrast, under carbon-abundant conditions (3, 6 and 9% CO₂), the microalgae priority switches to storing this surplus energy as triacylglycerols (TAGs) with the primary fatty acid channeled into these storage TAGs being the MUFA C18:1 [49]. This metabolic switch is explained by the C18 biosynthetic pathways. In this pathway, specific enzymes are required to create PUFAs: a delta-12 desaturase first converts C18:1 into C18:2, and then a delta-15 desaturase converts C18:2 into C18:3 [48]. The data shown in Table 3 provide evidence of the regulation of this pathway. Under high CO₂, the sharp drop in the final product (C18:3, from 39% to 11%) and the massive accumulation of its precursor (C18:1, from 7.6% to 40%) strongly implied that the high CO₂ concentration turned off these desaturase enzymes. This creates a metabolic bottleneck, halting the production of the membrane lipid C18:3 and causing the primary storage lipid C18:1 to accumulate.

If the algal biomass is targeted for biodiesel production, high-quality biodiesel feedstock should have a high concentration of MUFAs, such as C18:1, to ensure favorable cold-flow characteristics. At the same time, the feedstock should have low levels of PUFAs (C18:2 and C18:3) to guarantee oxidative stability [16,50]. Although PUFAs can enhance combustion properties because of their lower viscosity, they are more susceptible to oxidation, leading to reduced oxidative stability and overall fuel quality. Furthermore, elevated CO₂ aeration promotes the synthesis of SFA C18:0, which is known for its long hydrocarbon chains that release substantial energy upon combustion, thereby enhancing the calorific value [51]. Alongside the consistently detected C16:0, these saturated lipids may enhance biodiesel properties by increasing oxidation stability and cetane number [52]. This indicates that CO₂ aeration is required for biofuel production. As per the European Standards (EN 14214, 2004) for diesel engine quality, the amount of C18:3 and polyunsaturated acids with four or more double bonds in biodiesel is limited to a maximum of 12% and 1%, respectively, to ensure quality [53,54]. Therefore, the only condition meeting the 12% limit is 9% CO₂, while 3 and 6% CO₂ are very close to the limit and might be in the range with further improvement. However, if the target product is the omega-3 fatty acid C18:3, the data clearly shows that cultivation should occur under carbon-limiting conditions (0.04% CO₂ aeration) to maximize its yield. It should also be noted that biomass produced in AD as in this study is not suitable for food applications.

Based on the results attained in the first stage, 6% CO₂ concentration was chosen for the second stage of the experimental work (Sect. 3.4–3.6); this conditions resulted in highest biomass production, highest CO₂ fixation rate among all conditions, and comparable NH₄⁺-N and P removal compared to 3%. In the second stage different reactor designs were evaluated for optimal cultivation of *Chlorococcum* sp. in the same media.

Effect of reactor configuration on microalgae growth

Based on the initial assessment of various CO₂ levels, 6% CO₂ aeration was chosen mainly because of its superior biomass yield. This concentration was then used to evaluate the effectiveness of different reactors (BC, ALR, and BC with carriers) in terms of biomass production, nutrient removal, and biomass composition of *Chlorococcum* sp. Figure 4 presents the number of cells, biomass concentration and pH changes of *Chlorococcum* sp. using different reactor configurations for 12 days. As illustrated in Fig. 3C, from day 1 to day 12, the pH levels were stable, with average values of 7.28 ± 0.07 for BC, 7.23 ± 0.05 for ALR, and 7.18 ± 0.07 for BC with carriers. The maximum number of cells (81 × 10⁶ cells mL⁻¹) was obtained with microalgae grown in ALR on day 9, followed by BC (72.5 × 10⁶ cells mL⁻¹) and BC with carriers (72 × 10⁶ cells mL⁻¹) both on day 11 (Fig. 3B). Despite this, microalgae grown in BC yielded more biomass (0.96 ± 0.05 g L⁻¹) compared to ALR (0.86 ± 0.02 g L⁻¹) (Fig. 3A). This difference is attributed to the fact that the microalgae grown in ALR reaches the stationary phase earlier than the other reactors. This difference reflects the distinct hydrodynamic and mass-transfer characteristics of the two reactor types. The ALR provides strong internal circulation driven by the airlift loop, which enhances mixing, reduces cell sedimentation, and improves light exposure [55]. These conditions support rapid early growth (a higher biomass production than the others up to day 9), explaining why the ALR culture reached the stationary phase earlier than the BC. However, once the culture becomes dense, the ALR's flow pattern can lead to increased light attenuation and reduced effective illuminated volume, limiting further biomass accumulation.

In contrast, the BC exhibits slower initial growth but maintains a more stable growth phase for a longer period. The BC's larger illuminated surface area and gentler mixing can reduce photoinhibition and allow more uniform light penetration at higher biomass densities. This enables the BC to continue accumulating

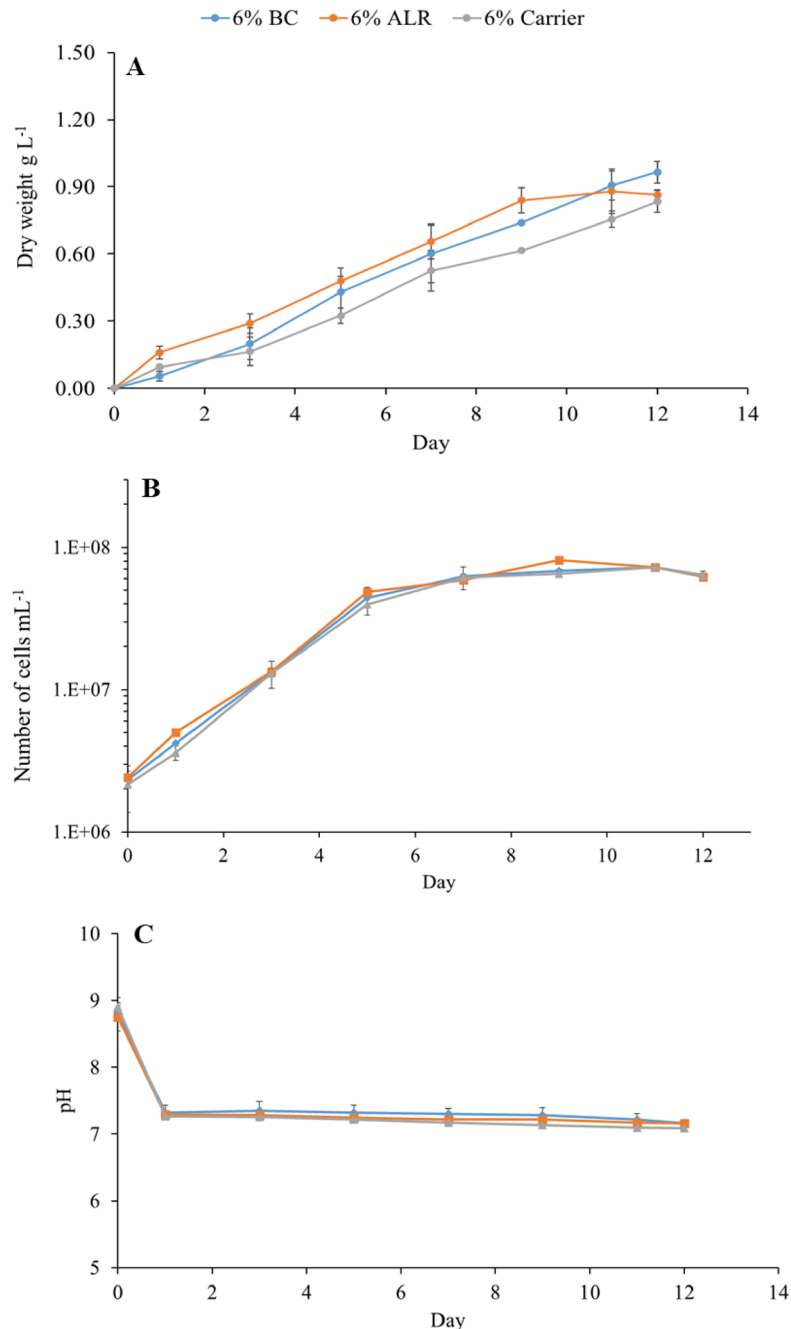


Fig. 4. Biomass concentration (A), number of cells (B), and pH changes (C) of *Chlorococcum* sp. cultures cultivated in anaerobic digestion effluents using different reactor configurations.

biomass even after the ALR culture has plateaued. Oncel and Sukan [56] reported that for *Spirulina platensis* cultivation using in BC and ALR, microalgae grown in the ALR photobioreactor produced a higher dry biomass weight concentration, achieving a maximum growth rate of 0.45 day^{-1} , whereas the microalgae grown in BC photobioreactor only reached a growth rate of 0.33 day^{-1} . It has also been noted that *Nannochloropsis* sp. achieved a higher cell concentration, resulting in improved growth when cultivated using an ALR compared to a BC, as the central tube in the ALR system provides a distinct flow pattern, superior light distribution, and more efficient mixing [23]. However, Uyar, Ali and Uyar [57] reported that *Chlorella sorokiniana* performed best in a BC photobioreactor when compared with a stirred tank and an ALR system. In their study, the BC equipped with a microporous sparger generated much smaller bubbles, resulting in significantly higher volumetric mass transfer compared to the ALR and stirred tank reactors, and ultimately superior growth (highest specific growth rate and biomass productivity).

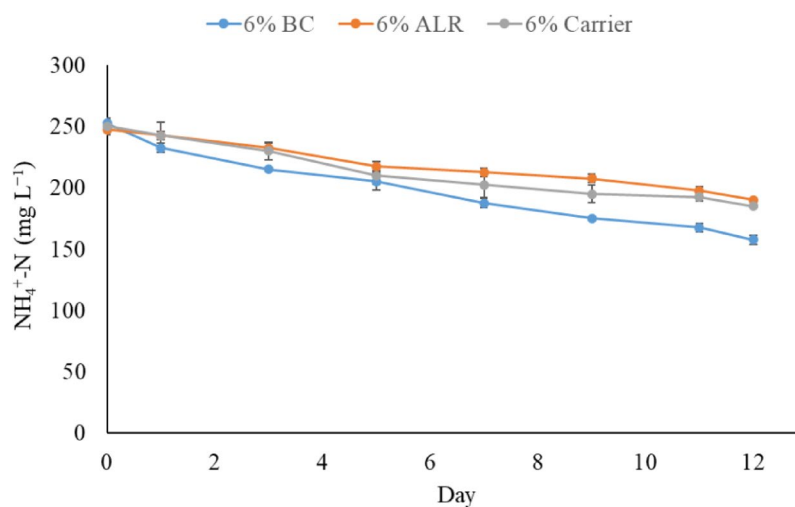


Fig. 5. Ammonium nitrogen removal by *Chlorococcum* sp. cultures cultivated in anaerobic digestion effluents using different reactor configurations.

CO ₂ (%)	Removal efficiency (%)		Productivity mg _{biomass} L ⁻¹ d ⁻¹	CO ₂ fixation rate mg _{CO₂} L ⁻¹ d ⁻¹
	NH ₄ ⁺ -N	P		
Reactors				
BC	37.61 ± 2.27 ^a	25.87 ± 0.48 ^a	65.00 ± 3.54 ^a	132.45 ± 5.18 ^a
ALR	23.22 ± 1.10 ^b	15.69 ± 2.18 ^b	67.5 ± 4.71 ^a	135.58 ± 12.4 ^a
Carrier	25.97 ± 2.09 ^b	16.79 ± 2.94 ^b	77.08 ± 5.3 ^a	155.49 ± 11.89 ^a

Table 4. Nutrient removal efficiency, biomass productivity, and CO₂ fixation rates using different reactor configurations. Values followed by different letters within the same column are significantly different (p value < 0.05).

Effect of reactor configuration on nutrient and CO₂ removal

Figure 5 illustrates the ammonium nitrogen removal for different reactor configurations over 12 days. Cultures cultivated in BC achieved better performance in ammonium removal during the whole cultivation period, while microalgae grown in ALR and BC with carrier showed comparable results. Table 4 shows the removal efficiency of NH₄⁺-N and P, biomass productivity, and CO₂ fixation rate of *Chlorococcum* sp. grown in different reactor configurations.

The microalgae grown in BC reactor achieved the highest removal rates for NH₄⁺-N and phosphorus, with 37.61% and 25.87%, respectively. Microalgae grown in ALR and BC containing carriers showed comparable performances in NH₄⁺-N and phosphorus removal, with no statistically significant differences observed. The biomass productivity ranged from 65 to 77.08 mg L⁻¹ d⁻¹, while the CO₂ fixation rate was between 132.45 and 155.49 mg CO₂ L⁻¹ d⁻¹. While both parameters led to comparable results across all configurations, BC with carriers reactor showed slightly higher CO₂ fixation rate (155.49 mg CO₂ L⁻¹ d⁻¹). This may be attributed to the presence of carriers, which could impede the release of CO₂ bubbles by prolonging their residence time in the liquid phase.

Effect of reactor configuration on biomass composition

The fatty acid composition, total FAMES, protein, carbohydrate, C/N ratio, ash and crude fat content of *Chlorococcum* sp. biomass after growth for 12 days using different reactors are presented in Table 5. The contents of individual fatty acids, total FAMES, carbohydrate, protein content, and C/N ratio were comparable across all configurations, indicating that the reactor design had no significant effect on these parameters. The finding that key biochemical components remained stable across all reactor configurations demonstrates metabolic robustness in *Chlorococcum* sp., and this stability is industrially advantageous. This demonstrates that the core metabolism of *Chlorococcum* sp. is not affected by the differing hydrodynamic and gas transfer environments, which is highly advantageous for industrial scale-up, as it allows reactor selection based on cost and productivity rather than concerns over product quality. Moreover, microalgae grown in BC produced significantly higher crude fat (1.98 ± 0.08) compared to other reactor configurations. However, a huge difference between crude fat and total FAMES content is clear, as shown in Table 5. This discrepancy arises from the extraction methods used. Crude fat was quantified using standard Soxhlet extraction with petroleum ether applied directly to intact, dried biomass. Because this method does not include any cell-disruption step, the solvent cannot effectively penetrate the thick cell wall of *Chlorococcum* sp. As a result, only a small fraction of easily extractable or free lipids, approximately 2%, is recovered. In contrast, the FAMES analysis involves transesterification, which chemically

Fatty acid profile (%)	Different reactor configurations (6% CO ₂)		
	BC	ALR	Carrier
C16:0 (palmitic acid)	18.11 ± 0.55	18.69 ± 1.33	18.49 ± 0.00
C16:1 (palmitoleic acid)	0.92 ± 0.11	0.87 ± 0.02	0.77 ± 0.14
C18:0 (stearic acid)	0.11 ± 0.00	0.13 ± 0.03	0.11 ± 0.03
C18:1 (oleic acid)	36.79 ± 1.02	34.22 ± 1.29	33.74 ± 0.35
C18:2 (linoleic acid)	25.79 ± 1.78	26.98 ± 0.12	26.93 ± 0.70
C18:3 (linolenic acid)	12.47 ± 0.26	13.07 ± 0.06	13.79 ± 0.54
Biomass (% of dry weight)			
Total FAMES	31.49 ± 0.13	30.44 ± 0.92	30.69 ± 1.35
Protein	39.19 ± 0.67	39.91 ± 0.33	39.94 ± 0.43
Carbohydrate	9.12 ± 0.64	9.98 ± 0.78	7.64 ± 0.50
C/N ratio	6.78 ± 0.01	6.55 ± 0.19	6.57 ± 0.02
Crude fat	1.98 ± 0.08	1.44 ± 0.50	1.64 ± 0.08
Ash	2.88 ± 0.35	2.69 ± 0.53	2.72 ± 0.012

Table 5. Fatty acids profile, total FAMES, protein, carbohydrate, C/N ratio, ash and crude fat content of the biomass using different reactor designs.

converts all saponifiable lipids (including membrane-bound and intracellular lipids) into measurable fatty acid methyl esters. Therefore, the total FAMES value reflects the full lipid pool, whereas the crude fat value represents only the solvent-accessible portion.

In comparison with previous studies, it was expected that the presence of carriers would enhance microalgal performance, as reported in previous studies where carriers improved nutrient uptake and overall biomass productivity [24,26]. For example, Serrano-Blanco, Zan, Harvey and Velasquez-Orta [25] observed a 2.8-fold increase in cell productivity when cultivating *Tetradismus obliquus* with suspended carriers. However, in our study, the inclusion of carriers did not lead to measurable improvements in biochemical composition or total FAMES production by *Chlorococcum* sp. This contrast suggests that the positive effects of carriers are species- and system-dependent, and it might be offset by the light shading effect caused by the carriers.

While microalgae-based systems are promising for reducing reliance on non-renewable resources, several factors still constrain their large-scale industrial application. High production costs, limited culture stability, susceptibility to inhibition, and the energy-intensive nature of harvesting remain major bottlenecks. In addition, the rigid algal cell wall often necessitates costly pretreatment steps, and regulatory uncertainties further complicate commercialization. Addressing these challenges is essential for enabling the effective scale-up of microalgal technologies and realizing their full contribution to a sustainable bioeconomy.

Conclusion

This study investigated the ability of the Nordic microalgal strain *Chlorococcum* sp. to grow and remove nutrients from municipal sewage sludge AD effluent using different CO₂ concentrations or reactor configurations. The results demonstrated that *Chlorococcum* sp. cultivated under 6% CO₂ aeration supported the highest biomass production, while maintaining nutrient removal comparable to 3% and 9%. Furthermore, elevated CO₂ levels promoted fatty acids accumulation, with total FAMES content ranging from 2.88% to 34.48% of dry biomass. The dominant fatty acids identified were C16:0, C18:1, C18:2, and C18:3. Moreover, CO₂ enriched aeration shifted the fatty acid profile from C18:3 toward C18:1, which may improve biodiesel quality. Reactor configurations influenced growth dynamics and nutrient removal. Growth in ALR achieved the highest cell density (81×10^6 cells mL⁻¹), while cultivation in BC yielded a greater biomass concentration (0.96 ± 0.05 g L⁻¹) and highest NH₄⁺-N and P removal (37.61% and 25.87%, respectively). Protein, carbohydrate, and FAMES content of the microalgae remained statistically consistent independent of the reactor types, indicating that reactor choice primarily affects growth kinetics and nutrient removal rather than biochemical composition. These findings underscore the importance of optimizing CO₂ levels and reactor design to maximize microalgal growth and achieve desired algal biomass composition for the intended application.

Data availability

The data that supports the findings of this study will be made available upon request.

Received: 30 January 2026; Accepted: 25 April 2026

Published online: 28 April 2026

References

- Pratap, B. et al. Wastewater generation and treatment by various eco-friendly technologies: Possible health hazards and further reuse for environmental safety. *Chemosphere* **313**, 137547 (2023).
- Ilango, V. & Sridharan, K. Significance of automation in water treatment processes, *Computational Automation for Water Security: Enhancing Water Quality Management* 2025, pp. 175–194.

3. Jiyane, P., Hoorzook, K. B. & van Rensburg, N. J. The state of wastewater treatment plants and how it is affecting the effluent discharge quality within the water bodies of Gauteng, Nature-Based Technologies for Wastewater Treatment and Bioenergy Production2025, pp. 139–152.
4. Waseem, M., Khan, M. U., Bokhary, A. & Ahring, B. K. Emerging trends in sewage sludge pretreatment: Enhancing treatment efficiency and sustainable waste management. *Clean. Water* **3**, 100080 (2025).
5. Ahmad, M. et al. Sequential Anaerobic/Aerobic Digestion for Enhanced Carbon/Nitrogen Removal and Cake Odor Reduction. *Water Environ. research: Res. publication Water Environ. Federation*. **88**, 2233–2244 (2016).
6. Song, Y. et al. The promising way to treat wastewater by microalgae: Approaches, mechanisms, applications and challenges. *J. Water Process. Eng.* **49**, 103012 (2022).
7. Hassan, L. H. S. Microalgal Treatment of Wastewater by Suspended and Immobilized Algal Systems: An Approach Contributing to Circular Bioeconomy, Green Technologies for Wastewater Treatment and Bioenergy Production2025, pp. 110–131.
8. Ivanova, J., Gigova, L. & Alexandrov, S. Successful practices for valorization of microalgal biomass for inclusion in circular economy. *South. Afr. J. Bot.* **175**, 408–425 (2024).
9. Elalami, D., Oukarroum, A. & Barakat, A. Anaerobic digestion and agronomic applications of microalgae for its sustainable valorization. *RSC Adv.* **11**, 26444–26462 (2021).
10. Mehariya, S. et al. Biopolymer production from biomass produced by Nordic microalgae grown in wastewater. *Bioresour. Technol.* **376**, 128901 (2023).
11. Yu, K. L. et al. Biochar production from microalgae cultivation through pyrolysis as a sustainable carbon sequestration and biorefinery approach. *Clean Technol. Environ. Policy*. **20**, 2047–2055 (2018).
12. Sarker, N. K. & Kaparaju, P. Microalgal wastewater treatment: A circular economy approach, Nature-Based Technologies for Wastewater Treatment and Bioenergy Production2025, pp. 153–172.
13. Chekanov, K., Schastnaya, E., Solovchenko, A. & Lobakova, E. Effects of CO₂ enrichment on primary photochemistry, growth and aeaxanthin accumulation in the chlorophyte *Haematococcus pluvialis*. *J. Photochem. Photobiol., B*. **171**, 58–66 (2017).
14. Aghaalipour, E., Akbulut, A. & Güllü, G. Carbon dioxide capture with microalgae species in continuous gas-supplied closed cultivation systems. *Biochem. Eng. J.* **163** (2020).
15. Fan, J. et al. Impacts of CO₂ concentration on growth, lipid accumulation, and carbon-concentrating-mechanism-related gene expression in oleaginous *Chlorella*. *Appl. Microbiol. Biotechnol.* **99**, 2451–2462 (2015).
16. Harwati, T. U., Willke, T. & Vorlop, K. D. Characterization of the lipid accumulation in a tropical freshwater microalgae *Chlorococcum* sp. *Bioresour. Technol.* **121**, 54–60 (2012).
17. Shin, C. Y., Noh, Y. J., Jeong, S. Y. & Kim, T. G. Characterization of cellular growth, CO₂ assimilation and neutral lipid production for 4 different algal species. *Microbiol. Biotechnol. Lett.* **48**, 547–555 (2021).
18. Ding, Y. D. et al. Dynamic behaviour of the CO₂ bubble in a bubble column bioreactor for microalgal cultivation. *Clean Technol. Environ. Policy*. **18**, 2039–2047 (2016).
19. Kalontarov, M., Doud, D. F. R., Jung, E. E., Angenent, L. T. & Erickson, D. In situ hollow fiber membrane facilitated CO₂ delivery to a cyanobacterium for enhanced productivity. *RSC Adv.* **3**, 13203–13209 (2013).
20. Hu, Z. M. et al. Enhancement of CO₂ transfer and carbon fixation by microalgae in photobioreactor. *Zhongguo Huanjing Kexue/China Environ. Sci.* **38**, 3967–3974 (2018).
21. Babcock, R. W., Wellbrock, A., Slenders, P. & Radway, J. C. Improving mass transfer in an inclined tubular photobioreactor. *J. Appl. Phycol.* **28**, 2195–2203 (2016).
22. Giannelli, L., Yamaji, H. & Katsuda, T. A numerical model for the quantification of light/dark cycles in microalgal cultures: Air-lift and bubble-column photobioreactor analysis by means of computational fluid dynamics. *J. Chem. Eng. Jpn.* **48**, 61–71 (2015).
23. Roncallo, O. P. et al. Comparison of Two Different Vertical Column Photobioreactors for the Cultivation of *Nannochloropsis* sp. *J. Energy Resour. Technol.* **135**, 011201 (2013).
24. Takabe, Y. et al. Effects of fluidised carriers on the community composition, settleability and energy production of indigenous microalgal consortia cultivated in treated wastewater. *Bioresour. Technol.* **381**, 129133 (2023).
25. Serrano-Blanco, S., Zan, R., Harvey, A. P. & Velasquez-Orta, S. B. Intensified microalgae production and development of microbial communities on suspended carriers and municipal wastewater. *J. Environ. Manage.* **370**, 122717 (2024).
26. Zhu, X. et al. Role of flow and mass transfer in photobioreactor: From bacteria locomotion to hydrogen production, International Heat Transfer Conference, pp. 251–256. (2018).
27. Mohammadkhani, G., Mahboubi, A., Plöhn, M., Funk, C. & Ylittervo, P. Total ammonia removal from anaerobic digestion effluents of municipal sewage sludge using Nordic microalgae. *Algal Res.* **84**, 103802 (2024).
28. Ferro, L., Gentili, F. G. & Funk, C. Isolation and characterization of microalgal strains for biomass production and wastewater reclamation in Northern Sweden. *Algal Res.* **32**, 44–53 (2018).
29. Prado Barragán, L. A., Figueroa, J. J. B., Rodríguez Durán, L. V., Aguilar González, C. N. & Hennigs, C. Chap. 7 - Fermentative Production Methods, in: P. Poltronieri, O.F. D’Urso (Eds.) *Biotransformation of Agricultural Waste and By-Products*, Elsevier2016, pp. 189–217.
30. Denovix, T. N. 222 Counting Algae Cells Using Intrinsic Chlorophyll Fluorescence, (2022).
31. Mehariya, S., Plöhn, M., Leon-Vaz, A., Patel, A. & Funk, C. Improving the content of high value compounds in Nordic *Desmodesmus* microalgal strains. *Bioresour. Technol.* **359**, 127445 (2022).
32. Cavonius, L. R., Carlsson, N. G. & Undeland, I. Quantification of total fatty acids in microalgae: comparison of extraction and transesterification methods. *Anal. Bioanal. Chem.* **406**, 7313–7322 (2014).
33. Phong, W. N. et al. Improving cell disruption efficiency to facilitate protein release from microalgae using chemical and mechanical integrated method. *Biochem. Eng. J.* **135**, 83–90 (2018).
34. Chen, W., Gao, L., Song, L., Sommerfeld, M. & Hu, Q. An improved phenol-sulfuric acid method for the quantitative measurement of total carbohydrates in algal biomass. *Algal Res.* **70**, 102986 (2023).
35. Jacob-Lopes, E., Scoparo, C. H. G., Lacerda, L. M. C. F. & Franco, T. T. Effect of light cycles (night/day) on CO₂ fixation and biomass production by microalgae in photobioreactors. *Chem. Eng. Process.* **48**, 306–310 (2009).
36. Gonçalves, A. L., Simões, M. & Pires, J. C. M. The effect of light supply on microalgal growth, CO₂ uptake and nutrient removal from wastewater. *Energy. Conv. Manag.* **85**, 530–536 (2014).
37. Liu, X. et al. Growth of *Chlorella vulgaris* and nutrient removal in the wastewater in response to intermittent carbon dioxide. *Chemosphere* **186**, 977–985 (2017).
38. Ying, K., Gilmour, D., Shi, Y. & Zimmerman, W. Growth Enhancement of *Dunaliella salina* by Microbubble Induced Airlift Loop Bioreactor (ALB)—The Relation between Mass Transfer and Growth Rate. *J. Biomaterials Nanobiotechnol.* **4**, 1–9 (2013).
39. Ritchie, R. J. & Sma-Air, S. Photosynthesis of an endolithic *Chlorococcum* alga (Chlorophyta, Chlorococcaceae) from travertine carbonate rocks of a tropical limestone Spring. *Appl. Phycol.* **3**, 1–15 (2022).
40. Nagabhushana, S., Yohannan, A. S. K., Malammanavar, S. G., Mookkan, P. & Iwar, K. Phytochemistry, bioactive potential and chemical characterization of culturable freshwater microalgae *Chlorococcum infusium* (Schrank) Meneghini. *Notulae Scientia Biologicae* **17** (2025).
41. Ledda, C., Romero Villegas, G. I., Adani, F. & Acien Fernández, F. G. Molina Grima, Utilization of centrate from wastewater treatment for the outdoor production of *Nannochloropsis gaditana* biomass at pilot-scale. *Algal Res.* **12**, 17–25 (2015).
42. Romero Villegas, G. I., Fiamengo, M., Acien Fernández, F. G., Molina, E. & Grima Outdoor production of microalgae biomass at pilot-scale in seawater using centrate as the nutrient source. *Algal Res.* **25**, 538–548 (2017).

43. Cano, R. et al. *Transforming Wastewater Treatment Plants in Bioenergy Factories Based on Microalgae Technology* (Social Science Research Network, 2022).
44. Robles-Heredia, J. C. et al. Evaluation of cell growth, nitrogen removal and lipid production by *Chlorella Vulgaris* to different conditions of aeration in two types of annular photobioreactors. *Revista Mexicana de Ingeniera Quim.* **15**, 361–377 (2016).
45. Nayak, M., Karemore, A. & Sen, R. Performance evaluation of microalgae for concomitant wastewater bioremediation, CO₂ biofixation and lipid biosynthesis for biodiesel application. *Algal Res.* **16**, 216–223 (2016).
46. Sun, Z. et al. Enhanced lipid accumulation of photoautotrophic microalgae by high-dose CO₂ mimics a heterotrophic characterization. *World J. Microbiol. Biotechnol.* **32**, 1–11 (2016).
47. Li, C. T. et al. Examining the impact of carbon dioxide levels and modulation of resulting hydrogen peroxide in *Chlorella vulgaris*. *Algal Res.* **60**, 102492 (2021).
48. Guschina, I. A. & Harwood, J. L. Lipids and lipid metabolism in eukaryotic algae. *Prog. Lipid Res.* **45**, 160–186 (2006).
49. Hu, Q. et al. Microalgal triacylglycerols as feedstocks for biofuel production: perspectives and advances. *Plant. journal: cell. Mol. biology.* **54**, 621–639 (2008).
50. Ciubota-Rosie, C., Ruiz, J. R., Ramos, M. J. & Pérez, Á. Biodiesel from *Camelina sativa*: A comprehensive characterisation. *Fuel* **105**, 572–577 (2013).
51. Rohit, M. V. & Mohan, S. V. Quantum yield and fatty acid profile variations with nutritional mode during microalgae cultivation. *Front. Bioeng. Biotechnol.* **6**, 111 (2018).
52. Islam, M. A. et al. Investigation of the effects of the fatty acid profile on fuel properties using a multi-criteria decision analysis. *Energy. Conv. Manag.* **98**, 340–347 (2015).
53. Knothe, G. Analyzing biodiesel: standards and other methods. *J. Am. Oil Chem. Soc.* **83**, 823–833 (2006).
54. En, J. U. S. *Automotive fuels. Fatty acid methyl esters (FAME) for diesel engines-Requirements and test methods* (Standardization Institute, 2004).
55. Monkonsit, S., Powtongsook, S. & Pavasant, P. Comparison between airlift photobioreactor and bubble column for *Skeletonema costatum* cultivation. *Eng. J.* **15**, 53–64 (2011).
56. Oncel, S. & Sukan, F. V. Comparison of two different pneumatically mixed column photobioreactors for the cultivation of *Arthrospira platensis* (*Spirulina platensis*). *Bioresour. Technol.* **99**, 4755–4760 (2008).
57. Uyar, B., Ali, M. D. & Uyar, G. E. O. Design parameters comparison of bubble column, airlift and stirred tank photobioreactors for microalgae production. *Bioprocess Biosyst. Eng.* **47**, 195–209 (2024).

Acknowledgements

The authors would like to express their appreciation to the University of Borås and Umeå University for their technical and financial support. They are also grateful to Borås Energy and Environment (Borås Energi och Miljö AB, Borås, Sweden) for providing the raw materials and offering technical assistance.

Author contributions

Ghasem Mohammadkhani: Investigation, methodology, data analyzing, writing - original draft; Amir Mahboubi: supervision, conceptualization, writing-review & editing; Christiane Funk: writing-review & editing and funding acquisition; Päivi Ylitervo: supervision, conceptualization, writing-review & editing and funding acquisition.

Funding

Open access funding provided by University of Borås. This project received financial support from ÅForsk (22–228). Additionally, the authors express gratitude for the funding support provided by ReSource (Energimyndigheten) to CF (P2024-00588) and to Bio4Energy (www.bio4energy.se) to CF.

Declarations

Declarations of generative AI use

Generative AI tools (Microsoft Copilot and Gemini 3 Flash) were used to improve grammar, clarity, and readability during the preparation of this manuscript. The authors take full responsibility for the content of the published article.

Conflict of interest

No conflicts of interest are disclosed by the authors.

Additional information

Correspondence and requests for materials should be addressed to G.M.

Reprints and permissions information is available at www.nature.com/reprints.

Publisher's note Springer Nature remains neutral with regard to jurisdictional claims in published maps and institutional affiliations.

Open Access This article is licensed under a Creative Commons Attribution 4.0 International License, which permits use, sharing, adaptation, distribution and reproduction in any medium or format, as long as you give appropriate credit to the original author(s) and the source, provide a link to the Creative Commons licence, and indicate if changes were made. The images or other third party material in this article are included in the article's Creative Commons licence, unless indicated otherwise in a credit line to the material. If material is not included in the article's Creative Commons licence and your intended use is not permitted by statutory regulation or exceeds the permitted use, you will need to obtain permission directly from the copyright holder. To view a copy of this licence, visit <http://creativecommons.org/licenses/by/4.0/>.

© The Author(s) 2026